JOC The Journal of Organic Chemistry

Article

pubs.acs.org/joc

Chiroptical Properties of Nona- and Dodecamethoxy Cryptophanes

Thierry Brotin,*,† Nicolas Vanthuyne,§ Dominique Cavagnat,‡ Laurent Ducasse,‡ and Thierry Buffeteau*,‡

†Laboratoire de Chimie de l'ENS Lyon (UMR 5182-CNRS), École Normale Supérieure de Lyon, 46 Allée d'Italie, 69364 Lyon, France

§Aix Marseille Université, Centrale Marseille, CNRS, iSm2 UMR 7313, 13397 Marseille, France

‡Institut des Sciences Moléculaires (UMR 5255-CNRS), Université de Bordeaux, 351 Cours de la Libération, 33405 Talence, France

S Supporting Information

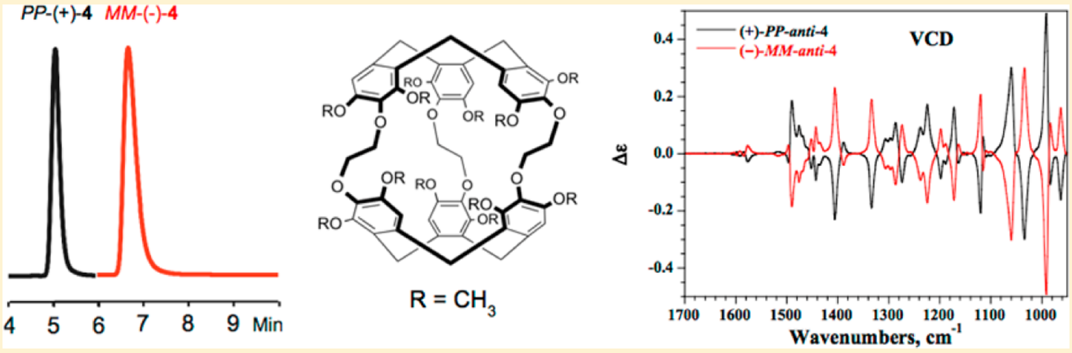

ABSTRACT: Enantiopure cryptophane derivatives bearing nine (**2**, **3**) and 12 (**4**) methoxy substituents attached on the six aromatic rings were separated by HPLC using chiral stationary phases. The chiroptical properties of compounds **2**–**4** were determined from polarimetry, electronic circular dichroism (ECD), and vibrational circular dichroism (VCD) experiments and were compared to those of cryptophane-A (**1**) derivative. ECD spectra of **1** and **4** were calculated by time-dependent density functional theory (TDDFT) to determine the absolute configuration (AC) of cryptophane derivatives. The (+)-*PP* absolute configuration was thus established for the *anti*-cryptophane-A (**1**) and its congeners **2** and **4**. VCD experiments associated with DFT calculations confirmed the (+)-*PP* configuration of *anti*-compounds **2** and **4** and established the (+)-*PM* configuration of the *syn*-**3** compound as well. This study revealed the preferential all-*trans* (*TTT*) conformation of the three ethylenedioxy linkers for the $CHCl_3$@**1**, $CHCl_3$@**3**, and $CHCl_3$@**4** complexes, whereas the *GTT* conformation was found the most favorable for the $CHCl_3$@**2** complex.

■ INTRODUCTION

Over the past 15 years cryptophane derivatives have attracted considerable attention because these hollow molecules can encapsulate elusive substrates (methane or xenon) or bind small chiral guest molecules.[1] Besides their interesting binding properties, cryptophane derivatives possess other interesting features. Indeed, most of the cryptophanes reported in the literature are inherently chiral molecules. The chirality of these systems comes from the particular arrangement of the three linkers that connect the two cyclotribenzylene (CTB) moieties. For instance, cryptophane-A (**1**) (see Scheme 1) possesses three ethylenedioxy linkers, whose helicoidal arrangement creates a cavity (V_{vdw} = 95 Å^3) with a chiral environment.[2] The cavity of cryptophane derivatives can accommodate chiral or achiral substrates whose size can be varied.[3] Moreover, it has been shown that cryptophane-C (a molecule congener of cryptophane-A) can bind differently the two enantiomers of bromochlorofluoromethane (CHFClBr). In this case, the enantioselective complexation has been detected using ^{1}H NMR spectroscopy.[4] More recently, several enantiopure cryptophanes soluble in organic solvents or in aqueous solution have been synthesized.[5] The synthesis of these molecules was possible thanks to the efficient separation of the two enantiomers of cryptophanol, a molecule congener of cryptophane-A bearing a single phenol group.[6] This approach

Scheme 1. Chemical Structure of *anti*-Cryptophane-A (1)[a]

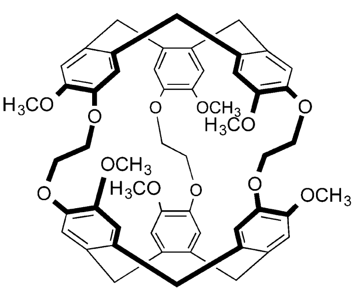

[a]Only the *MM* enantiomer is shown.

Received: March 17, 2014
Published: June 3, 2014

allowed us to isolate fair quantities of enantiopure materials and to study in detail the chiroptical properties of these new cryptophane derivatives in the presence or absence of guest molecules. For instance, cryptophane derivatives having D_3- or C_1-symmetry have been thoroughly investigated by electronic circular dichroism (ECD) and vibrational circular dichroism (VCD) spectroscopy under different experimental conditions (solvent, nature of the guest).[5,7] The use of VCD spectroscopy associated with density functional theory (DFT) calculations allowed the unambiguous determination of the absolute configuration (AC) of these new derivatives. These studies also provided important information on the conformation adopted by the host molecules in the presence or absence of guest molecules, especially when water was used as a solvent.

In this article, we investigate in detail the chiroptical properties of enantiopure cryptophane derivatives bearing nine (**2**, **3**) and 12 methoxy (**4**) substituents attached on the six aromatic rings (see Scheme 2). These compounds were recently prepared in their racemic form and constitute the only example reported in the literature of cryptophane derivatives bearing more than six substituents.[8] In contrast to cryptophane-A, the second ring-closing reaction leads to the synthesis of both *syn* and *anti* derivatives in moderate yields. The two diastereomers *anti*-**2** (C_3-symmetry) and *syn*-**3** (C_3-symmetry) are both chiral molecules. Similarly, molecule *anti*-**4** (D_3-symmetry) is chiral, but its diastereomer *syn*-**5** (C_{3h}-symmetry) is achiral. Consequently, compound **5** is of little interest in this study. The efficient separation of the two enantiomers of molecules **2**, **3**, and **4** by high performance liquid chromatography (HPLC) has given us the opportunity to investigate the chiroptical properties of these hosts by ECD and VCD spectroscopy. These chiroptical properties were compared with those previously reported for cryptophane-A (**1**) under similar experimental conditions. The AC of molecules **2**, **3**, and **4** has been determined from ECD and VCD associated with theoretical calculations (TDDFT for ECD and DFT for VCD). Combined, these spectroscopic data reveal how the presence of additional substituents attached on the phenyl rings modifies the overall chiroptical properties of cryptophane derivatives.

Scheme 2. Chemical Structures of *anti* and *syn* Cryptophanes Bearing Nine (2, 3) and 12 (4, 5) Methoxy Substituents

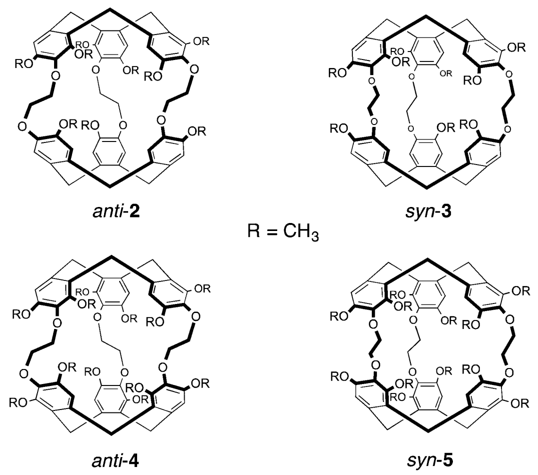

RESULTS AND DISCUSSION

Separation of Enantiomers of Compounds 2–4 by HPLC. Since the first synthesis of a cryptophane derivative in 1981 several approaches have been used to resolve cryptophane derivatives.[6,9] In this article, we have chosen to separate the two enantiomers of compounds **2**, **3**, and **4** by HPLC, using chiral stationary phases. This approach was found appropriate to provide quickly a fair amount of the two enantiomers of compounds **2–4**. This allowed us to perform polarimetry, ECD, and VCD experiments.

In this study, four chiral stationary phases (Chiralpak columns IA, IB, IC and ID, 250 mm × 4.6 mm) were tested to study their ability to separate efficiently the two enantiomers of compounds **2–4** (Supporting Information, S1). The results are summarized in Supporting Information (Tables 1–3 of S2 for the cryptophane derivatives *anti*-**2**, *syn*-**3**, and *anti*-**4**, respectively). For compound *anti*-**2**, an efficient separation of the two enantiomers was observed with the Chiralpak IB and Chiralpak IC columns using hexane/2-PrOH/$CHCl_3$ (50/30/20) and hexane/EtOH/$CHCl_3$ (50/30/20) mobile phases, respectively, for which very good resolution factors (Rs = 5.9 and Rs = 8.16) were measured (Supporting Information, S2: Table 1). Detection of the two enantiomers was achieved with a UV–vis detector connected to a polarimeter, giving the sign of the optical rotation in the eluent used for chromatography for each enantiomer (Figure 1, left, and Supporting Information, S3). It can be noticed that a change in the elution order is observed when the Chiralpak ID column is used as a stationary phase. For this study, the chiral column Chiralpak IB (250 mm × 10 mm) using a ternary mobile phase (hexane/2-PrOH/$CHCl_3$) has been chosen to achieve the preparative separation of the two enantiomers of *anti*-**2**. Thus, from 130 mg of racemic

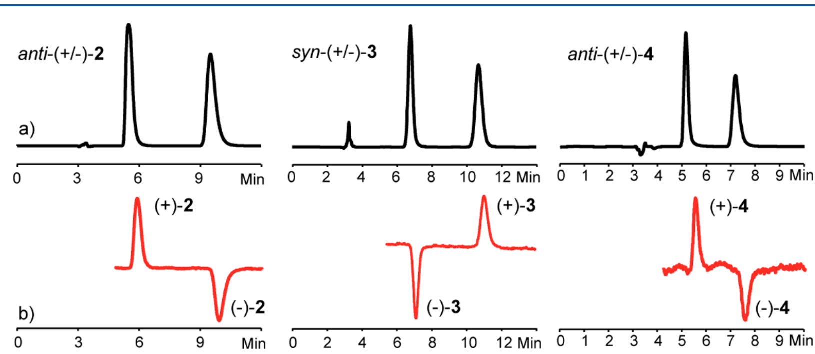

Figure 1. Separation of the two enantiomers of cryptophanes **2–4** by using analytical chiral HPLC columns (250 × 4.6 mm). *Anti*-(±)-**2** (Chiralpak IB; hexane/2-PrOH/$CHCl_3$ (50/30/20), 1 mL/min); *syn*-(±)-**3** (Chiralpak IA; hexane/EtOH/$CHCl_3$ (50/30/20), 1 mL/min); *anti*-(±)-**4** (Chiralpak ID; hexane/2-PrOH/$CHCl_3$ (50/30/20), 1 mL/min). a) detection by UV–vis (254 nm). b) detection by polarimetry.

dx.doi.org/10.1021/jo500621g | J. Org. Chem. 2014, 79, 6028–6036

Table 1. Optical Rotations (10^{-1} deg cm^2 g^{-1}) of the Two Enantiomers of Compounds 2−4 Recorded at 298 K at Several Wavelengths in $CHCl_3$[a]

compd	methoxy substituents	concn[b]	$[\alpha]_{589}^{25}$	$[\alpha]_{577}^{25}$	$[\alpha]_{546}^{25}$	$[\alpha]_{436}^{25}$	$[\alpha]_{365}^{25}$
(+)-*anti*-**2**	9	0.21	+187.3	+196.0	+227.1	+421.0	+774.2
(−)-*anti*-**2**	9	0.22	−185.0	−195.4	−225.6	−416.9	−771.0
(+)-*syn*-**3**	9	0.28	+35.0	+36.0	+42.6	+80.9	+168.3
(−)-*syn*-**3**	9	0.27	−34.2	−36.8	−42.7	−80.5	−169.0
(+)-*anti*-**4**	12	0.26	+95.3	+100.5	+117.0	+215.3	+387.3
(−)-*anti*-**4**	12	0.23	−97.2	−101.7	−117.3	−218.9	−389.3
(+)-*anti*-**1**[7a]	6	0.17	+269.0	+284.0	+326.5	+626.5	+1152.0
(−)-*anti*-**1**[7a]	6	0.13	−274.0	−288.0	−332.0	−623.0	−1154.0

[a]For comparison, optical rotations of the two enantiomers of cryptophane-A (**1**) are reported in the same solvent. [b]In g/100 mL.

material, 60 mg of (+)-*anti*-**2** (ee >99.5%) and 60 mg of (−)-*anti*-**2** (ee >99.5%) were isolated. Since evaporation of the mobile phase leads to yellow compounds, an additional purification step, consisting of a chromatography on silica gel (CH_2Cl_2/acetone, 90/10) followed by a crystallization in a $CHCl_3$/EtOH mixture, has been applied to both enantiomers. This additional purification step provides chemically pure enantiomers *anti*-(+)-**2** and *anti*-(−)-**2** as white crystalline materials with very high enantiomeric excess.

The same four chiral stationary phases were tested for the separation of the two enantiomers of compound *syn*-**3**. Very good resolution factors (around 6) were obtained with the Chiralpak IA and ID columns (250 mm × 4.6 mm) (Supporting Information, S2: Table 2). However, the Chiralpak IA column (250 mm × 10 mm) was found more appropriate to separate the two enantiomers of *syn*-**3**, since the elution time is significantly reduced and the mobile phase had to be modified in hexane/EtOH/$CHCl_3$ (30/40/30), due to the low solubility of *syn*-**3** in the mobile phase used for the analytical separation. Thus, from about 240 mg of *syn*-(±)-**3**, 110 mg of *syn*-(−)-**3** (ee >98.5%) and 110 mg of *syn*-(+)-**3** (ee >99.5%) were isolated, respectively (Figure 1, middle, and Supporting Information, S4). The same purification procedure as reported for compound **2** was applied to provide the two enantiomers of *syn*-**3** as white crystalline materials.

Finally, separation of *anti*-**4** enantiomers can be achieved on Chiralpak IC and Chiralpak ID (250 mm × 4.6 mm). Very good resolution factors have been observed with the two mobile phases used on Chiralpak ID, so this column was used for analytical separation (Supporting Information, S2: Table 3). The two enantiomers of compound *anti*-**4** were isolated using the Chiralpak IC column (250 mm × 10 mm) as a stationary phase. Thus, using a mixture of three solvents (hexane/2-PrOH/$CHCl_3$) as a mobile phase, 54 mg of *anti*-(+)-**4** (ee >99%) and 56 mg of *anti*-(−)-**4** (ee >99.5%) were obtained from 120 mg of *anti*-(±)-**4** (Figure 1, right, and Supporting Information, S5). As reported for compounds **2** and **3**, white crystalline compounds were obtained from an additional purification step.

Polarimetry and ECD Spectroscopy. The successful separation of enantiomers of **2**−**4** allowed us to investigate in detail the chiroptical properties of these compounds by polarimetry, ECD, and VCD techniques. Polarimetric measurements were performed in $CHCl_3$, and the optical rotation values of compounds **2**−**4** are reported in Table 1 at several wavelengths. As a comparison, the optical rotation values of the two enantiomers of cryptophane-A (**1**) are also reported. The results reveal a large difference in the magnitude of the optical rotatory power depending on the number of the methoxy groups attached to the phenyl rings. It can be noticed that, at a given wavelength, the larger the number of methoxy groups, the smaller the magnitude of the optical rotation values. Thus, going from cryptophane-A, possessing six methoxy groups as substituents, to compound *anti*-**4** bearing 12 methoxy groups, the $[\alpha]_{589}^{25}$ values decrease by a factor 3. Interestingly, intermediate $[\alpha]_{589}^{25}$ values were measured for the two enantiomers of the *anti*-**2** derivative bearing nine methoxy groups. The two enantiomers of compound *syn*-**3** represent a particular case in this series since the arrangement of the three linkers is different. Thus, the optical rotation values measured for (+)-**3** and (−)-**3** are the smallest among those reported in Table 1. The decrease of the optical rotation values with respect to those measured for compound **2**, bearing the same number of methoxy substituents, is about 5. The optical rotation values of cryptophane derivatives are very dependent on the arrangement of the three linkers (*anti* or *syn*) and on the number of the substituents attached on the phenyl rings.

Electronic circular dichroism (ECD) spectra of compounds **2**−**4** were measured in four different solvents ($CHCl_3$, CH_2Cl_2, THF, and 1,4-dioxane). Chloroform and dichloromethane solubilize cryptophanes **2**−**4** and can easily enter the cavity of these derivatives. The use of these two solvents gives rise to $CHCl_3$@cryptophane or CH_2Cl_2@cryptophane complexes. In contrast, 1,4-dioxane (V_{vdw} = 83 Å^3)[10] does not enter the cavity of compounds **2**−**4** at room temperature. Thus, cryptophane derivatives can be considered as guest-free in this solvent.[11] The situation appears less obvious in tetrahydrofuran (THF; V_{vdw} = 74 Å^3).[10] Indeed, when dissolved in tetrachloroethane-d_2 (V_{vdw} = 104 Å^3)[10] in the presence of an excess of THF, the ^{1}H NMR spectrum of *syn*-**3** reveals the presence of two high-field shifted signals (spectra not shown), which are characteristic of the presence of a THF molecule inside the cavity of *syn*-**3**. In contrast, these signals are not observed when the same experiment is performed at room temperature with compounds **2** and **4**.

As previously observed with cryptophane-A (**1**) and its relatives, the UV−vis spectra of compounds **2**−**4** reveal two broad bands in $CHCl_3$ (Supporting Information, S6). These two bands correspond to the two forbidden ^1L_a and ^1L_b transitions (Platt's notation) of the phenyl rings. The band of moderate intensity (7000−16000 L·mol^{-1}·cm^{-1}) located in the 260−310 nm region corresponds to the ^1L_b transition of the phenyl rings. The second band located at lower wavelength (230−260 nm), possessing a larger intensity (38000−43000 L·mol^{-1}·cm^{-1}), corresponds to the ^1L_a transition. It is noteworthy that the ^1L_b transition is particularly affected by the presence of additional methoxy groups attached on the phenyl rings. Indeed, the larger the number of methoxy groups attached on

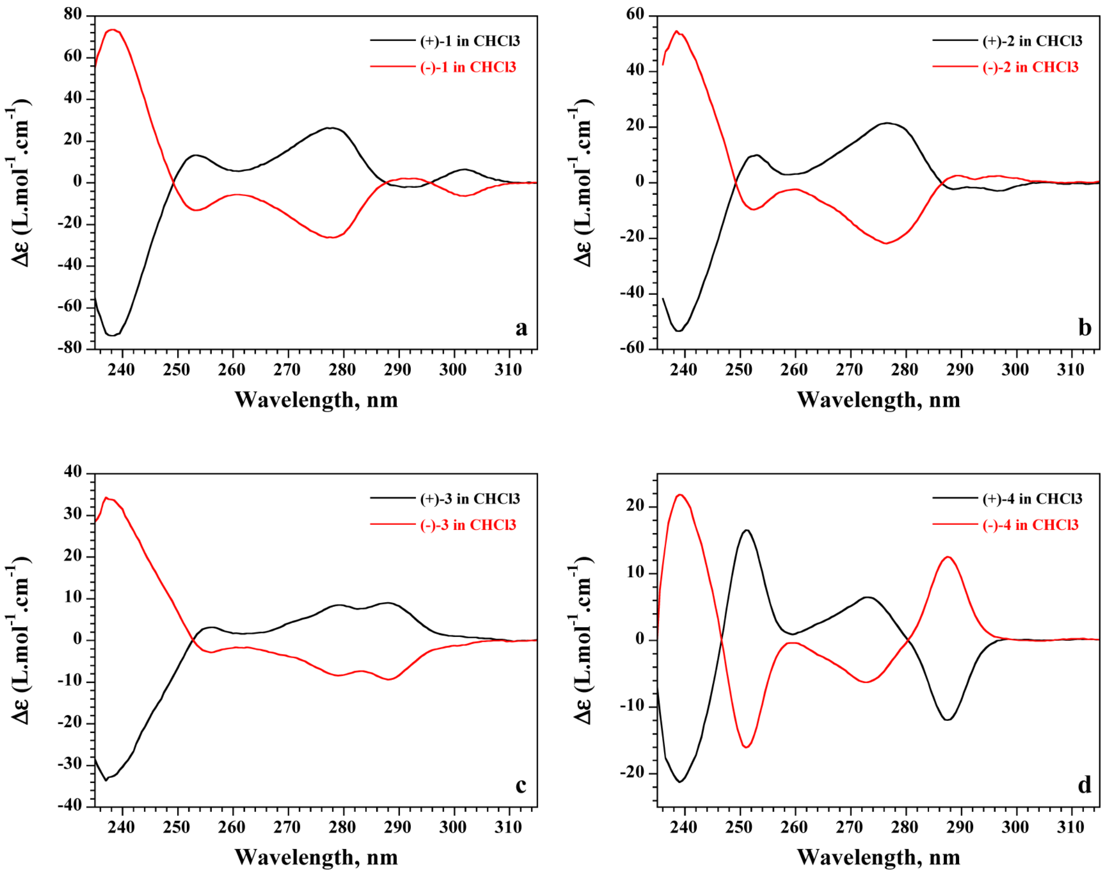

Figure 2. ECD spectra of compounds **1**−**4** recorded in $CHCl_3$ at 293 K. (a) *anti*-(+)-**1** (black spectrum) and *anti*-(−)-**1** (red spectrum). (b) *anti*-(+)-**2** (black spectrum) and *anti*-(−)-**2** (red spectrum). (c) *syn*-(+)-**3** (black spectrum) and *syn*-(−)-**3** (red spectrum). (d) *anti*-(+)-**4** (black spectrum) and *anti*-(−)-**4** (red spectrum).

the phenyl rings, the smaller the intensity of the ^1L_b transition. Moreover, a hypsochromic shift of the ^1L_b band is observed for compound **4** with respect to cryptophane-A. In contrast, the intensity of the ^1L_a band is less affected by the presence of additional methoxy substituents. A small bathochromic shift of this band is observed for compound **4**. The bathochromic and hypsochromic shifts of the ^1L_a and ^1L_b bands of compound **4** with respect to compound **1** are well reproduced by TDDFT calculations of the UV−vis spectra of these two cryptophanes, respectively (Supporting Information, S7).

The effect of additional methoxy substituents attached on the cryptophane skeleton for compounds **2** and **4** can be easily observed by comparing their ECD spectra with that of cryptophane-A (**1**), bearing a single methoxy substituent per phenyl ring. As shown in Figure 2, the ECD spectra of compounds **1**−**4** recorded in $CHCl_3$ solution exhibit spectral modifications in the ^1L_a and ^1L_b regions. Indeed, the shape and the intensity of ECD bands are strongly dependent on the studied compounds, especially for the ECD bands corresponding to the ^1L_b transition. For instance, the ECD spectrum of *anti*-(+)-**4** in the 260−315 nm region appears as positive−negative bisignate (from short to long wavelength), whereas, in the same region, the ECD spectrum of the *anti*-(+)-**1** and *anti*-(+)-**2** derivatives show a medium positive band associated with two weak negative−positive and negative-negative bands, respectively. The situation is even different for the *syn*-(+)-**3** derivative, since only positive ECD bands are observed in the ^1L_b region. In contrast, the two ECD bands of the ^1L_a transition, which appears as bisignate at shorter wavelength (230−260 nm), are less sensitive to substituent effects. Indeed, all of the (+)-**1**−**4** derivatives exhibit a negative−positive sequence in the 230−260 nm spectral range, even though a strong difference in intensity for the two bands can be observed for compounds **1**−**3**. This bisignate pattern is clearly observed for the two enantiomers of **4**, since the two components have similar intensity (Figure 2d). The bisignate patterns observed in the ^1L_a and ^1L_b region were analyzed in terms of exciton coupling between the transition dipole moments of the three aryl chromophores of the two CTB units.[12] The addition of substituents on the aryl groups produces rotations of the polarization directions of the ^1L_a and ^1L_b transition dipole moments, and consequently, different ECD spectra in the 230−310 nm region are expected for cryptophanes **1**−**4**. In a recent article, S. Abbate et al. have shown on simple optically active hexahelicenes that several ECD (or VCD) bands are dependent on the addition of a substituent, whereas others bands are invariant and are characteristic of the helicity of the compounds.[13] By analogy, the two ECD bands of the ^1L_a transition seems to be responsive for the structural chirality of the cryptophane derivatives, whereas the ECD bands in the ^1L_b region are substituent-sensitive.

The use of other solvents such as THF and 1,4-dioxane allowed us to have access to a larger spectral range. The extension of the spectral region (210 nm) gives access to an additional ECD band corresponding to the allowed ^1B_b transition (Supporting Information, S8). The intensity of the ECD band of the ^1B_b transition is significantly stronger than those corresponding to the ^1L_a and the ^1L_b transitions. In

dx.doi.org/10.1021/jo500621g | J. Org. Chem. 2014, 79, 6028−6036

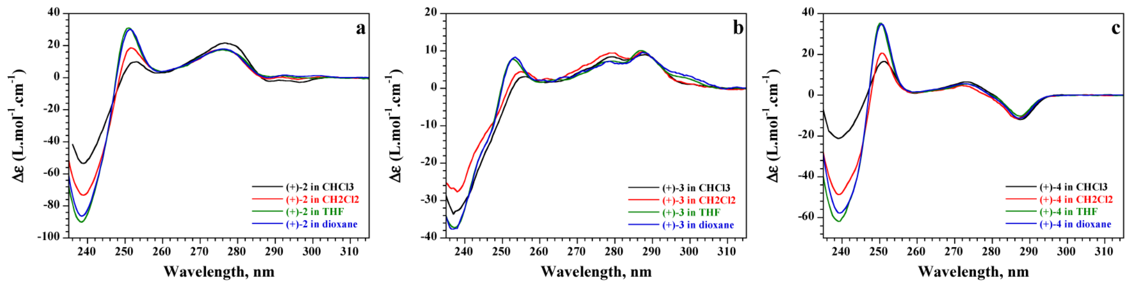

Figure 3. ECD spectra of compounds (a) (+)-**2**, (b) (+)-**3**, and (c) (+)-**4** recorded in various solvents at 293 K.

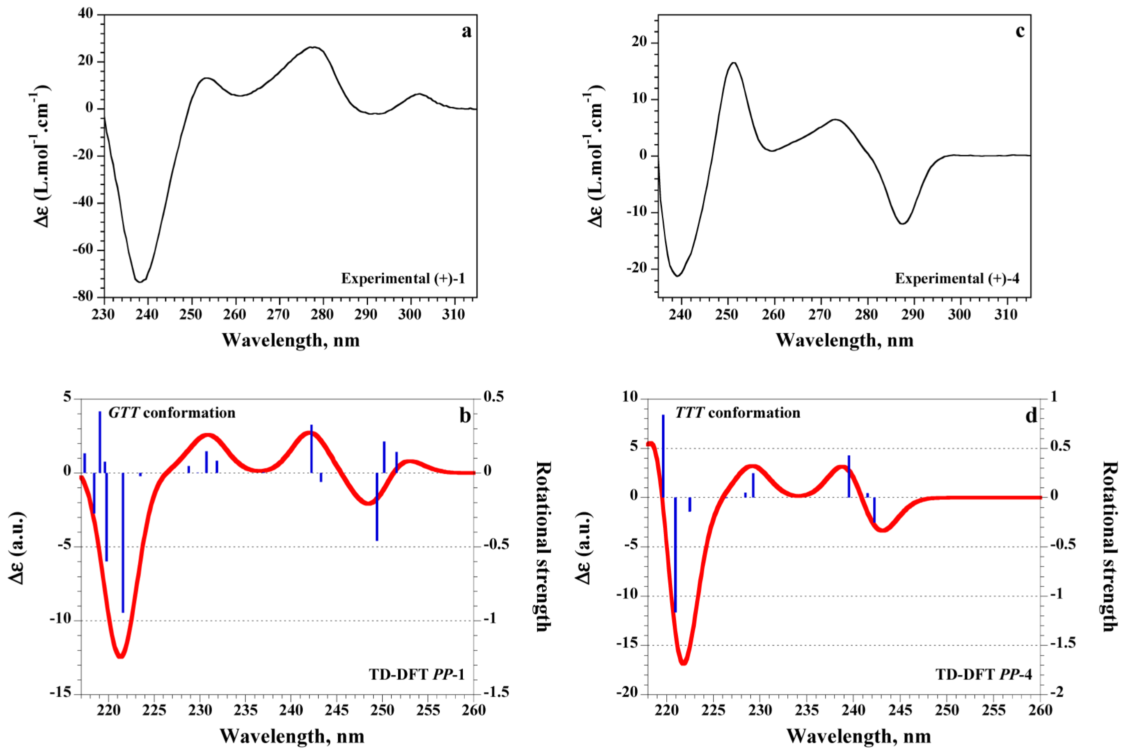

Figure 4. Comparison of the experimental ECD spectra of (a) (+)-**1** and (c) (+)-**4** compounds recorded in $CHCl_3$ solutions with the counterpart spectra calculated by TDDFT for the *PP* configuration considering (b) the *GTT* conformation of the three linkers for *PP*-**1** and (d) *TTT* conformation of the three linkers for *PP*-**4**. The rotational strengths (blue bars) should be multiplied by 10^{-40} erg·esu·cm/Gauss.

addition, as shown in Figure 3 (and Supporting Information, S9−S11), the change of the solvent leads to small but clear modifications of the ECD spectra, particularly in the ^1L_a region (230−260 nm). For instance, we observe a significant increase of the ECD bands for compounds (+)-(**2**) and (+)-(**4**) as well as the apparition of a well-defined negative−positive bisignate pattern. This spectral region is less affected for the (+)-(**3**) derivative. In addition, it is noteworthy that the ECD bands located at higher wavelength (^1L_b region) are weakly affected by the change of the solvent. This feature contrasts with the results previously reported for cryptophanes possessing a C_1-symmetry where a strong modification of the ECD spectra as a function of the nature of the solvent was noticed.[5a] The spectral modifications observed for compounds **2** and **4** can be interpreted in term of conformational change occurring upon encapsulation. In $CHCl_3$, the encapsulation of a chloroform molecule by hosts **2** and **4** leads to a rigid complex where the three linkers adopt preferentially an all-*trans* conformation. In the absence of efficient binding, the host molecules are certainly less constrained, favoring the *gauche* conformations of the linkers. It is noteworthy that the modifications of ECD spectra in various solvents are less important for host *syn*-(+)-**3**. This result can be explained by the spatial arrangement of the three linkers of the *syn* derivative, restricting to possibility of the hosts to modulate the cavity size in order to optimize their interaction with the guest. The modulation of the cavity size is certainly easier for *anti* derivatives due to the twist arrangement of the linkers, which can act as a spring.

The bisignate pattern observed in the ^1L_a region has been previously used to determine the absolute configuration (AC) of cryptophane-A (**1**) or hemicryptophane derivatives.[14] It has been found that the *PP* (respectively, *MM*) configuration[15] displays in the ^1L_a region a couplet structure with a negative−positive (respectively, positive−negative) sequence from short to long wavelength. By analogy with these results, the *PP* configuration can be assigned to the *anti*-(+)-**2** and *anti*-(+)-**4** compounds. In turn, the *MM* configuration can be assigned to the *anti*-(−)-**2** and *anti*-(−)-**4** compounds. To confirm these results and determine unambiguously the absolute configuration of *anti*-cryptophane-A derivatives, we have performed TDDFT calculations to predict for the first time the ECD spectra of *PP*-**1** and *PP*-**4** compounds. The comparison of the

dx.doi.org/10.1021/jo500621g | J. Org. Chem. 2014, 79, 6028−6036

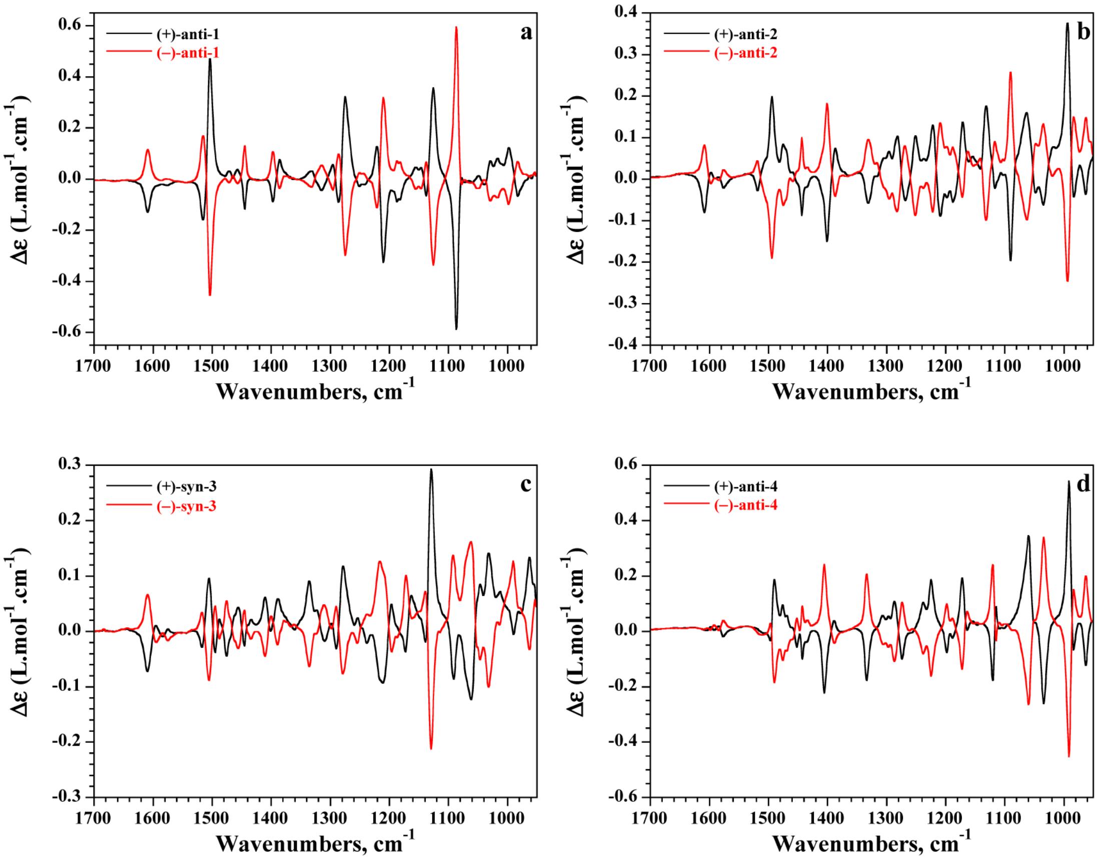

Figure 5. Experimental VCD spectra of the two enantiomers ((+) in black and (−) in red) of (a) *anti*-**1**, (b) *anti*-**2**, (c) *syn*-**3**, and (d) *anti*-**4** in $CDCl_3$ solution (20 mM, 250 μm path length).

experimental ECD spectra of (+)-**1** and (+)-**4** recorded in $CHCl_3$ solutions with the predicted ECD spectra for the *PP* configuration are presented in Figure 4 and in Supporting Information (S12). The TDDFT calculations were performed for the *trans,trans,trans* (*TTT*) and the *gauche,trans,trans* (*GTT*) conformations of the three ethylenedioxy linkers. First of all, we can note that the ECD contributions of the ^1L_a and ^1L_b transitions are calculated at lower wavelengths with respect to those observed in the experimental ECD spectra.[16] Nevertheless, the overall shape of the predicted ECD spectra reproduces fairly well the experimental ECD spectra. For example, the negative−positive and positive−negative couplets observed for the ^1L_a and ^1L_b transitions of (+)-**4**, respectively, are perfectly reproduced for the *PP* configuration of the cryptophane, confirming the *PP* configuration of *anti*-(+)-cryptophane-A derivatives. Finally, the positive contribution observed around 300 nm in the experimental ECD spectrum of (+)-**1** can be reproduced by TDDFT calculations, considering the *GTT* conformation of the three linkers (Figure 4b).

IR and VCD Spectroscopy. The chiroptical properties of enantiopure cryptophanes **1**−**4** were also investigated by vibrational circular dichroism (VCD). IR and VCD experiments of compounds **1**−**4** were performed in $CDCl_3$ solutions (0.020 M). The corresponding IR spectra are reported in Supporting Information (S13), whereas the VCD spectra in the 1700−950 cm^{-1} spectral range are presented in Figure 5. Most of the bands observed in the IR spectra of **1**−**4** were assigned for other cryptophane-A derivatives.[7a,b] The IR spectrum of *anti*-**2**, bearing nine methoxy substituents, is approximately the half-sum of the IR spectra of *anti*-**1** (cryptophane-A) and *anti*-**4**, bearing six and 12 methoxy substituents, respectively. This result indicates that the IR contributions of each CTB unit are additive and that the conformation of the ethylenedioxy linkers seems not to be affected by the number of methoxy substituents attached on the benzene rings. In a previous article, we have shown that the IR spectra of compounds **2**−**4** calculated at the DFT level reproduce, with a rather good agreement, the corresponding experimental spectra.[8] Thus, the spectral differences observed between the experimental IR spectra of compounds **1**, **2**, and **4** can be easily explained by the theoretical calculations. In addition, the small spectral differences between *anti*-**2** and *syn*-**3** diastereomers can be well reproduced by the DFT calculations, allowing the discrimination between the two compounds.

The chiroptical properties of cryptophane-A derivatives seem to be very dependent on the number of methoxy substituents and on the arrangement of the three linkers (*anti* or *syn*). Indeed, strong spectral modifications were observed in the VCD spectra of the four compounds **1**−**4**. For instance, the intensities of the bands due to the $\nu_{8b}C{=}C$ and $\nu_{19b}C{=}C$ stretching vibrations of the rings observed at 1608 and 1504 cm^{-1}, respectively, in the VCD spectra of **1** (Figure 5a), decrease strongly for compound **4**. In contrast, the band observed around 1400 cm^{-1}, due to the δ_sCH_3 bending modes of the methyl groups, increases significantly in the VCD spectra of **4** (Figure 5d). Moreover, new strong VCD bands appear below 1100 cm^{-1} in Figure 5d, coming from the coupling of the $\nu_sC{-}O{-}C$ stretching vibrations of additional methoxy substituents and ethylenedioxy linkers. As previously observed

 dx.doi.org/10.1021/jo500621g | J. Org. Chem. 2014, 79, 6028−6036

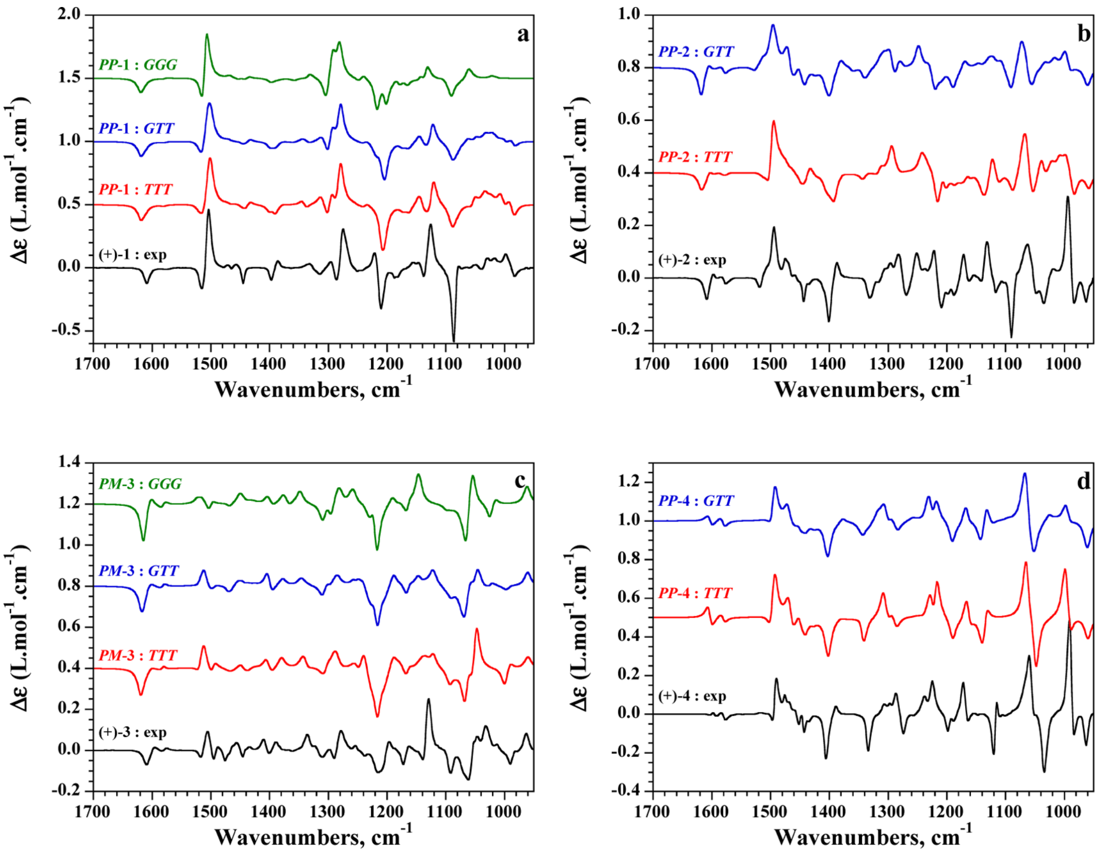

Figure 6. Comparison of experimental VCD spectra of (a) (+)-**1**, (b) (+)-**2**, (c) (+)-**3**, and (d) (+)-**4** recorded in $CDCl_3$ solution with calculated spectra at the B3PW91/6-31G** level for *TTT*, *GTT*, and *GGG* conformers of $CHCl_3$@*PP*-**1**, $CHCl_3$@*PP*-**2**, $CHCl_3$@*PM*-**3**, and $CHCl_3$@*PP*-**4** complexes.

for IR spectra, VCD spectra of *anti*-**2** are approximately the half-sum of the VCD spectra of *anti*-**1** and *anti*-**4**. It is noteworthy that the intensities of the major VCD bands are lower for compounds **2** and **4** than those measured for compound **1**. The VCD signal still decreases for *syn*-**3**. The same tendency has been observed from polarimetric and ECD experiments.

To confirm the absolute configuration of cryptophane-A derivatives and to obtain additional information on the conformation of the linkers, ab initio calculations at the DFT level were performed for compounds **1**−**4**. The geometries of $CHCl_3$@*PP*-**1**, $CHCl_3$@*PP*-**2**, $CHCl_3$@*PM*-**3**,[17] and $CHCl_3$@*PP*-**4** complexes were optimized at the B3PW91/6-31G** level, and harmonic vibrational frequencies were calculated at the same level. Calculations were performed for the *TTT*, *GTT*, and *GGG* conformations of the three ethylenedioxy linkers. The electronic and the Gibbs energies are reported in Supporting Information (S14). On the basis of the ab initio predicted Gibbs free energies, it can be concluded that the *TTT* conformer is the most favorable for $CHCl_3$@**1**−**4** complexes. This result is not surprising due to the better size matching between the chloroform (ca. 72 Å^3) and the cryptophane cavity in its all-*trans* conformation (ca. 95 Å^3). Nevertheless, we cannot exclude the presence of the *GTT* conformer for *anti*-**1** and *anti*-**2** since the difference Gibbs free energies (ΔG) calculated for this conformer is very low. Moreover, this conformation of the aliphatic bridges has been determined from the X-ray structure of crystalline $CHCl_3$@*PP*-**1** complex.[18] In addition, as shown above, TDDFT calculation of the ECD spectrum of $CHCl_3$@*PP*-**1** complex reveals the presence of the *GTT* conformer.

The VCD spectra calculated at the B3PW91/6-31G** level for *TTT*, *GTT*, and *GGG* conformers of $CHCl_3$@*PP*-**1**, $CHCl_3$@*PP*-**2**, $CHCl_3$@*PM*-**3**, and $CHCl_3$@*PP*-**4** complexes are compared in Figure 6 to the experimental spectra of (+)-**1**−**4** recorded in chloroform solution. For the three *anti* compounds, the spectra calculated for the *PP* configuration reproduce the sign of most of the bands observed in the experimental VCD spectra, confirming the absolute configuration (+)-*PP* of *anti*-cryptophane derivatives. The comparison of experimental and predicted VCD spectra of *syn*-**3** allowed the determination of the (+)-*PM* configuration for this compound. Concerning the conformation of the linkers, the spectra calculated for the *TTT* conformer of $CHCl_3$@*PP*-**1** and $CHCl_3$@*PP*-**4** complexes reproduce fairly well the sign and the intensity of the bands observed in the counterpart experimental VCD spectra. A quite good agreement for the *GTT* conformer of $CHCl_3$@*PP*-**1** complex is also observed. For the $CHCl_3$@*PP*-**2** complex, a good agreement between theoretical calculations and experiment is obtained for the *GTT* conformer. Finally, for the $CHCl_3$@*PM*-**3** complex, the DFT calculations do not show a good correlation with the VCD experimental spectrum, even though the *TTT* conformer seems to be the most favorable. This peculiar behavior is certainly due to the fact that cryptophane **3** is the only molecule of the series that does not display a three-dimentional helical structure.

■ CONCLUSION

In this article, we report a detailed study of the chiroptical properties of cryptophanes **2**–**4**, bearing nine (**2**, **3**) and 12 (**4**) methoxy substituents attached on the six aromatic rings. These chiroptical properties are compared to those of the cryptophane-A (**1**), bearing six methoxy substituents. The two enantiomers of cryptophanes **2**–**4** were successfully separated by HPLC using chiral stationary phases. The optical rotation values of cryptophanes **1**–**4** are found to be very dependent on the arrangement of the three linkers (*anti* or *syn*) and on the number of the substituents attached on the phenyl rings. These values strongly decrease for highly substituted cryptophanes and for the *syn* compound. This study also shows that ECD spectroscopy is a very useful technique to investigate chiroptical properties of cryptophanes since ECD spectra of compounds **1**–**4** exhibit significant spectral modifications in the ^1L_a and ^1L_b regions. Indeed, the shape of the ECD bands is strongly dependent on the studied compounds in the ^1L_b region, as well as the intensity of the couplet observed in the ^1L_a region. ECD spectra of **1** and **4** were calculated for the first time, by time-dependent density functional theory, allowing the determination of the (+)-*PP* configuration for *anti*-cryptophane-A derivatives. This (+)-*PP* configuration for *anti*-cryptophane-A derivatives has been confirmed by VCD experiments associated with DFT calculations. In addition, the VCD/DFT approach has established the (+)-*PM* configuration of the *syn*-**3** compound and has provided complementary information about the conformation of the ethylenedioxy linkers for the chloroform-cryptophane complexes. Thus, $CHCl_3$@**1**, $CHCl_3$@**3**, and $CHCl_3$@**4** complexes have revealed a preferential all-*trans* (*TTT*) conformation of the three linkers, whereas the *GTT* conformation was found the most favorable for the $CHCl_3$@**2** complex.

■ EXPERIMENTAL SECTION

Synthesis. The synthetic route to obtain enantiopure cryptophane **1** was previously reported.[6,7a] Cryptophanes **2**–**5** were synthesized as racemic compounds according to a known procedure.[8] The optical resolution of compounds **2**–**4** has been achieved by HPLC using a chiral stationary phase as described below. ^{1}H NMR spectra and HRMS of (+)-*anti*-**2**, (−)-*anti*-**2**, (+)-*syn*-**3**, (−)-*syn*-**3**, (+)-*anti*-**4**, and (−)-*anti*-**4** are identical to those previously reported for the counterpart racemic compounds (Supporting Information, S15–S20).[8]

Chiral Separation by HPLC. The chiral separation of compound *anti*-**2** was conducted on a semipreparative Chiralpak IB column (250 mm × 10 mm), thermostated at 30 °C using hexane/2-PrOH/$CHCl_3$ (50/30/20) as mobile phase. The flow rate was 5 mL/min. UV–vis detection was performed at 254 nm; 60 injections (250 μL) every 13 min were necessary to separate the two enantiomers of the racemic mixture of *anti*-**2** (130 mg).

The chiral separation of compound *syn*-**3** was conducted on a semipreparative Chiralpak IA column (250 mm × 10 mm), thermostated at 30 °C using hexane/EtOH/$CHCl_3$ (30/40/30) as mobile phase. The flow rate was 5 mL/min; 260 injections (1000 μL) every 4 min were necessary to separate the two enantiomers of the racemic mixture of *syn*-**3** (240 mg).

The chiral separation of compound *anti*-**4** was performed on a semipreparative Chiralpak IC column (250 mm × 10 mm), thermostated at 30 °C using hexane/2-PrOH/$CHCl_3$ (50/30/20) as mobile phase. The flow rate was 5 mL/min; 100 injections (300 μL) every 8.5 min were necessary to separate the two enantiomers of the racemic mixture of *anti*-**4** (130 mg).

The determination of the enantiomeric excess (ee) was then determined by chiral HPLC, injecting separately each purified enantiomer (+)-*anti*-**2**, (−)-*anti*-**2**, (+)-*syn*-**3**, (−)-*syn*-**3**, (+)-*anti*-**4**, and (−)-*anti*-**4**. A chiroptical detector (polarimeter) was used to assign the sign for each peak.[19] Since the evaporation of the mobile phase leads to yellow materials for all purified compounds, an additional purification on silica gel (CH_2Cl_2/acetone, 90/10) followed by a recrystallization step ($CHCl_3$/EtOH) was necessary.

Polarimetric, UV–vis, and ECD Measurements. Optical rotations of compounds **2**–**4** were measured in $CHCl_3$ at several wavelengths on a polarimeter with a 100 mm cell thermostated at 25 °C. UV–vis and ECD spectra were recorded in four solvents ($CHCl_3$, CH_2Cl_2, THF, and 1,4-dioxane) at room temperature with a 0.2 cm (or 1 cm) path length quartz cell. The concentration of compounds **2**–**4** was taken in the range 2×10^{-5} to 9×10^{-5} M. Spectra were recorded in the 220–400 nm wavelength range with a 0.5 nm increment and a 1 s integration time. Spectra were processed with standard spectrometer software, baseline corrected, and slightly smoothed by using a third-order least-squares polynomial fit. Spectral units were expressed in difference of molar extinction coefficients.

IR and VCD Measurements. The infrared and VCD spectra were recorded with a FTIR spectrometer equipped with a VCD optical bench.[20] IR absorption and VCD spectra were recorded at a resolution of 4 cm^{-1}, by coadding 50 scans and 24,000 scans (8 h acquisition time), respectively. Samples were held in a variable path length cell with BaF_2 windows. IR and VCD spectra of the two enantiomers of compounds **1**–**4** were measured in $CDCl_3$ solvent at a concentration of 0.020 M and at a path length of 250 μm. In all experiments, the photoelastic modulator was adjusted for a maximum efficiency at 1400 cm^{-1}. Calculations were done with the standard spectrometer software, using Happ and Genzel apodization, de-Haseth phase correction, and a zero-filling factor of 1. Calibration spectra were recorded using a birefringent plate (CdSe) and a second BaF_2 wire grid polarizer, following the experimental procedure previously published.[21] Finally, in the presented IR spectra, the solvent absorption was subtracted out.

DFT and TDDFT Calculations. The geometry optimizations, vibrational frequencies and absorption intensities were calculated by the Gaussian 09 program[22] on the DELL cluster of the MCIA computing center of the University Bordeaux I. Calculations of the optimized geometry of $CHCl_3$@*PP*-**1**, $CHCl_3$@*PP*-**2**, $CHCl_3$@*PM*-**3**, and $CHCl_3$@*PP*-**4** complexes were performed at the density functional theory level using B3PW91 functional and 6-31G** basis set. Calculations were performed for the *TTT*, *GTT*, and *GGG* conformations of the three ethylenedioxy linkers. Vibrational frequencies and IR intensities were calculated at the same level of theory. For comparison to experiment, the calculated frequencies were scaled by 0.968, and the calculated intensities were converted to Lorentzian bands with a half-width of 7 cm^{-1}.

The UV–vis (excitation energies and associated oscillator strengths) and ECD spectra (excitation energies and rotational strengths) were calculated by time-dependent density functional theory (TDDFT) using the MPW1K functional containing 42.8% of HF exchange[23] and the 6-31+G** basis set. The calculations were performed using the Gaussian 09 package,[22] taking into account the solvent effects within the integral equation formalism of the polarizable continuum model (IEFPCM).[24] Other functionals/basis sets were used, but the MPW1*K*/6-31+G** approach was found to give reliable results against the overall shape of the UV–vis and ECD spectra. In particular, the ECD spectra calculated using a small basis, such as the 6-31G* basis set, does not compare well with experiment, showing that it is quite important to introduce polarization functions. For comparison to experiment, each transition of a UV–vis (or ECD) spectrum has been enlarged using a Gaussian function having a full width at half-maximum (fwhm) of 0.1 eV (0.05 eV for ECD).

■ ASSOCIATED CONTENT

Ⓢ Supporting Information

Separation of the two enantiomers of **2**–**4** by HPLC using different chiral stationary phases. UV–vis spectra of **1**–**4** recorded at 293 K in $CHCl_3$. UV–vis spectra of compounds **1** and **4** calculated by TDDFT for the *PP* configuration and the *TTT* conformation of the three ethylenedioxy linkers. ECD spectra of the two enantiomers of **1**−**4** recorded at 293 K in CH_2Cl_2, THF, and 1,4-dioxane. ECD spectra of compound **1** calculated by TDDFT for the *PP* configuration and the *GTT* conformation of the three ethylenedioxy linkers. Experimental IR spectra of (+)-**1**−**4**. Conformations and energies of $CHCl_3$@*PP*-**1**, $CHCl_3$@*PP*-**2**, $CHCl_3$@*PM*-**3**, and $CHCl_3$@*PP*-**4** complexes calculated at the B3PW91/6-31G** level. ^1H NMR spectra of the two enantiomers of compounds **2**−**4** recorded at 298 K in $CDCl_3$ solution. This material is available free of charge via the Internet at http://pubs.acs.org.

■ AUTHOR INFORMATION

Corresponding Authors

*E-mail: thierry.brotin@ens-lyon.fr.

*E-mail: t.buffeteau@ism.u-bordeaux1.fr.

Notes

The authors declare no competing financial interest.

■ ACKNOWLEDGMENTS

We thank Dr. James Cochrane for his critical reading of the article. The authors are indebted to the CNRS (Chemistry Department) and to Région Aquitaine for financial support in VCD equipment and also acknowledge computational facilities provided by the MCIA (Mésocentre de Calcul Intensif Aquitain) of the Université de Bordeaux and of the Université de Pau et des Pays de l'Adour, financed by the "Conseil Régional d'Aquitaine" and the French Ministry of Research and Technology.

■ REFERENCES

(1) (a) Collet, A. *Tetrahedron* **1987**, *43*, 5725−5759. (b) Brotin, T.; Dutasta, J.-P. *Chem. Rev.* **2009**, *109*, 88−130.

(2) Gabard, J.; Collet, A. *J. Chem. Soc. Chem. Comm.* **1981**, 1137−1139.

(3) Collet, A.; Dutasta, J.-P.; Lozach, B.; Canceill, J. *Top. Curr. Chem.* **1993**, *165*, 103−129.

(4) Canceill, J.; Lacombe, L.; Collet, A. *J. Am. Chem. Soc.* **1985**, *107*, 6993−6996.

(5) (a) Cavagnat, D.; Buffeteau, T.; Brotin, T. *J. Org. Chem.* **2008**, *73*, 66−75. (b) Bouchet, A.; Brotin, T.; Cavagnat, D.; Buffeteau, T. *Chem.—Eur. J.* **2010**, *16*, 4507−4518.

(6) Brotin, T.; Barbe, R.; Darzac, M.; Dutasta, J.-P. *Chem.—Eur. J.* **2003**, *9*, 5784−5792.

(7) (a) Brotin, T.; Cavagnat, D.; Dutasta, J.-P.; Buffeteau, T. *J. Am. Chem. Soc.* **2006**, *128*, 5533−5540. (b) Brotin, T.; Cavagnat, D.; Buffeteau, T. *J. Phys. Chem. A* **2008**, *112*, 8464−8470. (c) Bouchet, A.; Brotin, T.; Linares, M.; Agren, H.; Cavagnat, D.; Buffeteau, T. *J. Org. Chem.* **2011**, *76*, 1372−1383. (d) Bouchet, A.; Brotin, T.; Linares, M.; Agren, H.; Cavagnat, D.; Buffeteau, T. *J. Org. Chem.* **2011**, *76*, 4178−4181. (e) Bouchet, A.; Brotin, T.; Linares, M.; Cavagnat, D.; Buffeteau, T. *J. Org. Chem.* **2011**, *76*, 7816−7825.

(8) Brotin, T.; Cavagnat, D.; Jeanneau, E.; Buffeteau, T. *J. Org. Chem.* **2013**, *78*, 6143−6153.

(9) Tambute, A.; Canceill, J.; Collet, A. *Bull. Chem. Soc. Jpn.* **1989**, *62*, 1390−1392.

(10) Zhao, Y. H.; Abraham, M. H.; Zissimos, A. M. *J. Org. Chem.* **2003**, *68*, 7368−7373.

(11) We cannot exclude the presence of dissolved gases (nitrogen, molecular oxygen, etc.) in the cavity of these compounds. Nevertheless, these molecules are not expected to interact strongly with cryptophanes or to modify the conformation of the three linkers.

(12) (a) Canceill, J.; Collet, A.; Gabard, J.; Gottarelli, G.; Spada, G. *J. Am. Chem. Soc.* **1985**, *107*, 1299−1308. (b) Andraud, C.; Garcia, C.; Collet, A. In *Circular Dichroism: Principles and Applications*, 2nd ed.; Berova, N., Nakanishi, K., Woody, R. W.; Wiley-VCH: New York, 2000; Chapter 13, pp 383−395.

(13) Abbate, S.; Longhi, G.; Lebon, F.; Castiglioni, E.; Superchi, S.; Pisani, L.; Fontana, F.; Torricelli, F.; Caronna, T.; Villani, C.; Sabia, R.; Tommasini, M.; Lucotti, A.; Mendola, D.; Mele, A.; Lightner, D. A. *J. Phys. Chem. C* **2014**, *118*, 1682−1695.

(14) (a) Canceill, J.; Collet, A.; Gottarelli, G.; Palmieri, P. *J. Am. Chem. Soc.* **1987**, *109*, 6454−6464. (b) Perraud, O.; Raytchev, P. D.; Martinez, A.; Dutasta, J.-P. *Chirality* **2010**, *22*, 885−888.

(15) IUPAC 1968 Tentative Rules, Section E, Fundamental Stereochemistry in *J. Org. Chem.* **1970**, *35*, 2849−2867. See also: Collet, A.; Gabard, G.; Jacques, J.; Césario, M.; Guilhem, J.; Pascard, C. *J. Chem. Soc., Perkin Trans. 1* **1981**, 1630−1638.

(16) The calculated UV−vis excitation energies were blue-shifted by 20−45 nm compared to experiment. Using other functionals decreases this difference, but the shape of the spectra is quite different from the experimental one.

(17) For *PM* configuration, *P* corresponds to the configuration of the CTB unit bearing three methoxy substituents.

(18) (a) Cavagnat, D.; Brotin, T.; Bruneel, J.-L.; Dutasta, J.-P.; Thozet, A.; Perrin, M.; Guillaume, F. *J. Phys. Chem. B* **2004**, *108*, 5572−5581. (b) Taratula, O.; Hill, P. A.; Khan, N. S.; Carroll, P. J.; Dmochowski, I. J. *Nat. Commun.* **2010**, *148*, 1−7.

(19) Vanthuyne, N.; Roussel, C. *Top. Curr. Chem.* **2013**, *340*, 107−151.

(20) Buffeteau, T.; Lagugné-Labarthet, F.; Sourrisseau, C. *Appl. Spectrosc.* **2005**, *59*, 732−745.

(21) Nafie, L. A.; Vidrine, D. W. In *Fourier Transform Infrared Spectroscopy*; Ferraro, J. R., Basile, L. J., Eds.; Academic Press: New York, 1982; Vol. 3, pp 83−123.

(22) Frisch, M. J.; Trucks, G. W.; Schlegel, H. B.; Scuseria, G. E.; Robb, M. A.; Cheeseman, J. R.; Scalmani, G.; Barone, V.; Mennucci, B.; Petersson, G. A.; Nakatsuji, H.; Caricato, M.; Li, X.; Hratchian, H. P.; Izmaylov, A. F.; Bloino, J.; Zheng, G.; Sonnenberg, J. L.; Hada, M.; Ehara, M.; Toyota, K.; Fukuda, R.; Hasegawa, J.; Ishida, M.; Nakajima, T.; Honda, Y.; Kitao, O.; Nakai, H.; Vreven, T.; Montgomery, Jr., J. A.; Peralta, J. E.; Ogliaro, F.; Bearpark, M.; Heyd, J. J.; Brothers, E.; Kudin, K. N.; Staroverov, V. N.; Kobayashi, R.; Normand, J.; Raghavachari, K.; Rendell, A.; Burant, J. C.; Iyengar, S. S.; Tomasi, J.; Cossi, M.; Rega, N.; Millam, N. J.; Klene, M.; Knox, J. E.; Cross, J. B.; Bakken, V.; Adamo, C.; Jaramillo, J.; Gomperts, R.; Stratmann, R. E.; Yazyev, O.; Austin, A. J.; Cammi, R.; Pomelli, C.; Ochterski, J. W.; Martin, R. L.; Morokuma, K.; Zakrzewski, V. G.; Voth, G. A.; Salvador, P.; Dannenberg, J. J.; Dapprich, S.; Daniels, A. D.; Farkas, Ö.; Foresman, J. B.; Ortiz, J. V.; Cioslowski, J.; Fox, D. J. *Gaussian 09, revision A.1*, Gaussian Inc.: Wallingford, CT, 2009.

(23) Lynch, B. J.; Fast, P. L.; Harris, M.; Truhlar, D. G. *J. Phys. Chem. A* **2000**, *104*, 4811−4815.

(24) (a) Tomasi, J.; Persico, M. *Chem. Rev.* **1994**, *94*, 2027−2094. (b) Tomasi, J.; Mennucci, B.; Cammi, R. *Chem. Rev.* **2005**, *105*, 2999−3094.